Received: 8 November 2021 | Revised: 18 January 2022 | Accepted: 23 February 2022

DOI: 10.1111/omi.12364

ORIGINAL ARTICLE

WILEY

Streptococcus mutans cell division protein FtsZ has higher GTPase and polymerization activities in acidic environment

Yuxing Chen[1] | Yongliang Li[2] | Chongyang Yuan[1] | Shujun Liu[3] | Fengjiao Xin[3] | Xuliang Deng[2] | Xiaoyan Wang[1]

[1]Department of Cardiology and Endodontology & National Clinical Research Center for Oral Disease, School and Hospital of Stomatology, Peking University, Beijing, P. R. China

[2]Department of Geriatric Dentistry, School and Hospital of Stomatology, Peking University, Beijing, P. R. China

[3]Laboratory of Biomanufacturing and Food Engineering, Institute of Food Science and Technology, Chinese Academy of Agricultural Sciences, Beijing, P. R. China

Correspondence
Xiaoyan Wang, Department of Cardiology and Endodontology, Peking University School and Hospital of Stomatology, No.22, Zhongguancun south street, Beijing, P. R. China.
Email: wangxiaoyan@pkuss.bjmu.edu.cn
Xuliang Deng, Department of Geriatric Dentistry, Peking University Hospital of Stomatology, No.22, Zhongguancun south street, Beijing, P. R. China.
Email: kqdengxuliang@bjmu.edu.cn

Yuxing Chen and Yongliang Li contributed equally to the work.

Funding information
National Natural Science Foundation of China, Grant/Award Numbers: 81991501, 82001039; China Postdoctoral Science Foundation, Grant/Award Number: 2020M680265; Young Elite Scientist Sponsorship Program by CAST, Grant/Award Number: 2019QNRC001 to YL.L; Beijing Natural Science Foundation : 7222220

Abstract

The acid tolerance of *Streptococcus mutans* plays an important role in its cariogenic process. *Streptococcus mutans* initiates a powerful transcriptional and physiological adaptation mechanism, eventually shielding the cellular machinery from acid damage and contributing to bacterial survival under acidic stress conditions. Although *S. mutans* contains complex regulatory systems, existing studies have shown that *S. mutans*, unlike *Escherichia coli*, cannot maintain a neutral intracellular environment. As the pH of the extracellular environment decreases, the intracellular pH decreases in parallel. There is insufficient knowledge regarding the acid resistance of the intracellular proteins of *S. mutans*, particularly when it comes to the key cytoskeletal division protein FtsZ. In this study, the data showed that *S. mutans* had similar cell division progress in acidic and neutral environments. The splitting position was in the middle of cells, and the cytoplasm was divided evenly in the acidic environment. Additionally, the tread milling velocity of *S. mutans* FtsZ in the middle of cells was not affected by the acidic environment. *Streptococcus mutans* FtsZ had higher GTPase activity in pH 6.0 buffer than in the neutral environment. Furthermore, the polymerization of *S. mutans* FtsZ in the acidic environment was more robust than that in the neutral environment. After two particular amino acids of *S. mutans*, FtsZ amino acids were mutated (E88K, L269K), the polymerization of *S. mutans* FtsZ in the acidic environment was significantly reduced. Overall, *S. mutans* FtsZ exhibited higher functional activity in pH 6.0 buffer in vitro. The acid resistance of *S. mutans* FtsZ is affected by its particular amino acids.

KEYWORDS
FtsZ, GTPase, polymerization, *Streptococcus mutans*

1 | INTRODUCTION

Streptococcus mutans is thought to be the significant pathogen associated with dental caries. Its capacity to ferment a series of dietary carbohydrates can quickly drop extracellular pH levels, ultimately leading to tooth decay. To grow at a low pH, *S. mutans* initiates the acid tolerance response, a powerful transcriptional and physiological adaptation mechanism involving the induction of pathways that contribute to changes in cytoplasmic buffering and membrane fatty acid composition (Baker et al., 2017; Matsui & Cvitkovitch, 2010), eventually shielding

the cellular machinery from acid damage and contributing to bacterial survival under acidic stress conditions. With various cellular processes involved in the acid tolerance response, *S. mutans* can maintain growth and cell division at a pH of 5.5 (Lemos et al., 2019). Meanwhile under this circumstance, demineralization occurs on enamel surface and initiates the progression of caries.

Escherichia coli can maintain an intracellular pH of 7.2 to 7.8 in a pH 5.0 to 9.0 environment, thus, ensuring normal cell division and proliferation (Slonczewski et al., 1981). To regulate intracellular pH, the acid tolerance mechanism of *E. coli* to regulate intracellular pH is mainly achieved by amino acid-dependent decarboxylases and their counter transport protein systems, that is, glutamate-, arginine-, and lysine-dependent decarboxylase systems (Lund et al., 2014). Although *S. mutans* contains complex regulatory systems, such as the F-ATPase proton pump, the agmatine deiminase system, and the branched-chain amino acid biosynthesis mechanism. However, *S. mutans*, unlike *E. coli*, cannot neutralize its intracellular environment (Baker et al., 2017; Nogales et al., 1998). As the pH of the extracellular environment of *S. mutans* decreases, the intracellular pH decreases in parallel (Iwami et al., 2002). Owing to the environment around *S. mutans* in biofilm being about pH 3.5–5.5, despite *S. mutans* having the ability to maintain internal pH at 0.5 to 1.0 units above the external environment, its intracellular environment is acidic (Bender et al., 1986; Lemos et al., 2019).

Cell division is a fundamental process that has to be executed precisely in all living organisms (Mahone & Goley, 2020). Most bacteria propagate by binary fission, a cytoplasmic division process mediated mainly by the divisome. The divisome contains dozens of different proteins localized in the middle of the cell in a ring-like structure (Erickson et al., 2010). FtsZ is one of the core proteins in the division complex and was first localized to the bacterial cell division site (Erickson et al., 2010). FtsZ hydrolyzes GTP and polymerizes itself to filaments by binding GTP, composing a ring-like structure "Z-ring" at the splitting site (Bramhill & Thompson, 1994; De Boer et al., 1992). As a scaffold, the "Z-ring" recruits other division-associated proteins such as cytoplasmic localization proteins, endosomal or intermembrane localization proteins, to form the divisome in turn. In addition, FtsZ filaments exhibit a GTPase activity-dependent dynamic movement in vivo, regulating or influencing the rate of cell wall synthesis and, thus, the rate of the division in *E. coli* (Yang et al., 2017). In vitro, the GTPase activity of *E. coli* FtsZ decreases when the pH is below 6.8, while its GTPase activity is almost completely lost when the pH reaches 5.5 in vitro, suggesting an acidic environment with low pH impairs the function of *E. coli* FtsZ (Mueller et al., 2019).

However, how an acidic intracellular environment affects the function of *S. mutans* FtsZ remains unknown. Therefore, the purpose of our study was to determine whether *S. mutans* FtsZ has a unique mechanism of acid resistance. To do this, we used a mNeongreen fluorescent reporter tagged with *S. mutans* FtsZ to study its function in an acidic environment and then we analyzed its tread milling velocity. We tested GTP hydrolysis rates and polymerization activity of *S. mutans* FtsZ at different pH levels (pH 5.0–7.5) in vitro. Furthermore, site-specific mutations of *S. mutans* FtsZ were made via a quick-change strategy to identify unique amino acids, which was critical to acid tolerance.

2 | MATERIALS AND METHODS

2.1 | Bacterial strains and cultivation

The standard strain of *S. mutans* (UA159) and all derived strains used in this study are listed in Table 1. For *S. mutans* FtsZ_mNeongreen, which was tagged with a fluorescent protein, we used the IFDC2 system to select the correct mutation (Xie et al., 2011). First, UA159 was cultured at 37°C in the Todd—Hewitt medium with 0.3% Yeast Extract (THY) overnight. Then, the overnight culture was diluted (1:100) in THY and incubated for 2 h (OD600 = 0.2—0.3) in a 5% CO_2 incubator. Three DNA cassettes, including *ftsZ*, *IFDC2*, and *ftsZ*-downstream, were ligated using Q5 DNA polymerase by fusion polymerase chain reaction (PCR). The competence stimulating peptide and fusion PCR products were mixed in 500 μL of strain culture and incubated for 2 h. Brain Heart Infusion (BHI) agar plates with erythromycin (12 μg/mL) were used to select antibiotic-resistant colonies. Sanger sequencing was used to verify sequence accuracy. Second, after FtsZ, mNeongreen tag, and FtsZ-downstream were ligated by fusion PCR, homologous recombination was conducted to generate *S. mutans* FtsZ_mNeongreen. The BHI plates with 4 mg/mL p-cl-Phe were used to select colonies for the second transformation. Following sequence verification by Sanger sequencing, we ascertain the sequence is correct.

2.2 | Determination of growth curve and doubling time

Streptococcus mutans and *Streptococcus gordonii* were cultured in chemically defined medium with 0.1% Yeast Extract medium (CDY) and diluted to 10^5 colony forming units per milliliter into a 15 mL centrifuge tube in a 37°C 5% CO_2 incubator (Van De Rijn & Kessler, 1980). And the CDY medium with different pHs for different groups were made with 1 M HCl. Following vortex, 300 μL culture was transferred to one well of a standard 96-well plate every 1 h; every group has three duplicated wells. The OD600 value of each well was recorded by Multimode Plate Reader (EnSpire, PerkinElmer), wells with medium only (without bacteria) were used as blanks. The bacterial growth curves were drawn using Prism 8. Doubling time analysis was performed using the open-source R language.

2.3 | Fluorescence microscopy

Streptococcus mutans UA159 was grown in CDY medium at 37°C, 5% CO_2 for 16 h. The overnight culture was diluted (1:100) in CDY medium with a resulting pH of 7.4 or 5.0, respectively. Then, the *S. mutans* in the different pH values were incubated at 37°C, 5% CO_2 for 6 h (pH 7.4) or 10 h (pH 5.0) until OD600 = 0.4—0.5 was achieved. The culture was stained with FM 4–64 dye (50 μg/mL; Thermo Fisher Scientific) at room temperature for 5 min and followed by imaging.

TABLE 1 Bacterial strains and plasmids used in this study

Strains/Plasmid	Major characteristics	References
S.mutans UA159	wild-type	
S.gordonii ATCC10558	wild-type	
FtsZ-mNeongreen	UA159; Pzx9::FtsZ-mNeongreen, Str^R	This study
pET28a-SmFtsZ	*E.coli* BL21(DE3), $Kana^R$	This study
pET28a-EcFtsZ	*E.coli* BL21(DE3), $Kana^R$	This study
pET28a-SmFtsZ_mut E88D	*E. coli* BL21(DE3), $Kana^R$	This study
pET28a-SmFtsZ_mut S110T	*E. coli* BL21(DE3), $Kana^R$	This study
pET28a-SmFtsZ_mut N168D	*E. coli* BL21(DE3), $Kana^R$	This study
pET28a-SmFtsZ_mut N189D	*E. coli* BL21(DE3), $Kana^R$	This study
pET28a-SmFtsZ_mut Y247S	*E. coli* BL21(DE3), $Kana^R$	This study
pET28a-SmFtsZ_mut L269F	*E. coli* BL21(DE3), $Kana^R$	This study
pET28a-SmFtsZ_mut E88A	*E. coli* BL21(DE3), $Kana^R$	This study
pET28a-SmFtsZ_mut L269A	*E. coli* BL21(DE3), $Kana^R$	This study
pET28a-SmFtsZ_mut E88K	*E. coli* BL21(DE3), $Kana^R$	This study
pET28a-SmFtsZ_mut L269K	*E. coli* BL21(DE3), $Kana^R$	This study

2.4 | Snapshotting images of FtsZ

Streptococcus mutans FtsZ_mNeongreen was grown in CDY medium at 37°C for 16 h. The overnight culture was diluted (1:100) in CDY medium with a resulting pH of 7.4 or 5.0, respectively. Then, the *S. mutans* in the different pH values were incubated at 37°C for 6 h (pH 7.4) or 10 h (pH 5.0) until OD600 = 0.4–0.5 was achieved. The culture was diluted again (1:100) and grown under the same conditions for 2.5 h (pH 7.4) and 5 h (pH 5.0) until OD600 = 0.1–0.2 was achieved. Cells were centrifuged for harvest (1500 × *g* for 3 min), washed three times with phosphate-buffered saline (PBS), and then resuspended in PBS. Then, 1.5% low-melting agarose was used to load cells on a microslide.

Streptococcus mutans FtsZ_mNeongreen was imaged in 600 frames with an exposure time of 10 min N-STORM system (Nikon, Tokyo, Japan) equipped with a 100 × oil total internal reflection fluorescence (TIRF) objective lens (Nikon Plan Apo, 1.49 NA) (Yang et al., 2017), the Andor-897 EMCCD platform (Andor, Belfast, Northern Ireland), a laser source (405, 488, 561, and 647 nm), and 1.5 × magnification optics. Nis-Elements AR software (Nikon) was used to analyze the images.

2.5 | Imaging the dynamics of *S. mutans* FtsZ_mNeongreen

It is a breakthrough to be able to use the N-STORM microscope for imaging near-TIRF illumination pictures (Yang et al., 2017). We were able to collect the dynamic condition of FtsZ_mNeongreen easily. FtsZ_mNeongreen was excited by the 488 nm laser; and the exposure time was 0.165 s, and the interval time was 0.495 s.

2.6 | Transmission electron microscope analysis

Streptococcus mutans was grown in BHI (pH 7.4 and 5.0) until OD600 = ~0.4 was achieved. Cells were centrifuged for harvest (3220 × *g* for 15 min), washed with PBS once, and then fixed in 2% paraformaldehyde/2.5% glutaraldehyde at room temperature for 1 h. Again, cells were washed with PBS, fixed in 1% osmium tetroxide (Polysciences) for 1 h, and then rinsed in water before en-bloc staining for 1 h with 1% aqueous uranyl acetate. All samples were washed in water and dehydrated in a graded series of ethanol followed by embedding in Eponate 12 resin. Sections ~90 nm were prepared, stained with uranyl acetate and lead citrate, and viewed under a JEOL 1400 EX transmission electron microscope (De et al., 2018).

2.7 | Protein expression

The *ftsZ* genes from *S.mutans* UA159 and *E.coli* ATCC 8739 were cloned into the pET-28a vector separately with different restriction sites (NcoI and XhoI, NdeI and XhoI) to construct expressive plasmids, which were named pET28a-SmFtsZ and pET28a-EcFtsZ (oligonucleotide primers used in this study were listed in Table 2). For protein expression, plasmids were transformed into *E.coli* BL21 (DE3). The expression strains were cultured in lysogeny broth medium with kanamycin (50 μg/mL) for 4 h (OD600 = 0.6–0.8) in an incubator at 37°C and 200 rpm. Then, the incubator's temperature was cooled to 16°C and IPTG (0.2 mM) was added to the culture.

After an additional 16 h of growth, cells were collected by centrifugation at 4°C for 10 min (5000 *g*). Lysis buffer (150 mM NaCl, Tris-HCl pH 8.0, 1 mM $MgCl_2$, 1 μM phenylmethylsulfonyl fluoride, 0.1 mg/mL lysosome, and 1 μg/mL DNaseI) was used to resuspend all the cell pellets.

TABLE 2 Oligonucleotide primers used in this study

Primers	Sequence	Function
FtsZ_E.coli-NdeI-F-28a	ggaattcCATATGATGTTTGAACCAATGGAACTTACC	*E. coli* FtsZ
Cy_ftsZ_E.coli-Xho1-R	CCCTCGAGTTAATCAGCTTGCTTACGCAGG	
FtsZ_Sm-NcoI-F 1	catgCcATGGCATTTTCATTTGATGCAG	S. mutans FtsZ
FtsZ_Sm-XhoI-R 3	ccgCTCGAGACGATTCTTAAAGAAAGGAGG	
smFtsZmut-E86D-F1	GTAAAGCTGCTGAAGAAAGCgatGAAGCTTTGACAGAAGCACTTACTG	Mutation E88D
smFtsZmut-E86D-R1	CAGTAAGTGCTTCTGTCAAAGCTTCatcGCTTTCTTCAGCAGCTTTAC	
smFtsZmut-S108T-F2	CTGCTGGTATGGGTGGTGGTaccGGTACGGGAGCCGCT	Mutation S110T
smFtsZmut-S108T-R2	AGCGGCTCCCGTACCggtACCACCACCCATACCAGCAG	
smFtsZmut-N166D-F3	ATACGCTCCTTATTATTTCAAATgatAATCTACTTGAAATTGTTGACA	Mutation N168D
smFtsZmut-N166D-R3	TGTCAACAATTTCAAGTAGATTatcATTTGAAATAATAAGGAGCGTAT	
smFtsZmut-N187D-F4	TGAAGCACTCAGTGAAGCTGATgatGTTCTTCGCCAAGGTGTTCAGG	Mutation N189D
smFtsZmut-N187D-R4	CCTGAACACCTTGGCGAAGAACatcATCAGCTTCACTGAGTGCTTCA	
smFtsZmut-Y245S-F5	GCTGCTCGCAAGGCGATCagcTCACCACTTCTTGAGAC	Mutation Y247S
smFtsZmut-Y245S-R5	GTCTCAAGAAGTGGTGAgctGATCGCCTTGCGAGCAGC	
smFtsZmut-L268F-F6	TTGTCAATGTTACCGGCGGCtttGATATGACGCTGACAGAAGC	Mutation L269F
smFtsZmut-L268F-R6	GCTTCTGTCAGCGTCATATCaaaGCCGCCGGTAACATTGACAA	
smFtsZmut-E86A-F10	GTAAAGCTGCTGAAGAAAGCgcaGAAGCTTTGACAGAAGCACTTACTG	Mutation E88A
smFtsZmut-E86A-R10	CAGTAAGTGCTTCTGTCAAAGCTTCtgcGCTTTCTTCAGCAGCTTTAC	
smFtsZmut-L268A-F12	GTCAATGTTACCGGCGGCgcaGATATGACGCTGACAGAAG	Mutation L269A
smFtsZmut-L268A-R12	CTTCTGTCAGCGTCATATCtgcGCCGCCGGTAACATTGAC	
smFtsZmut-E86K-F13	GTAAAGCTGCTGAAGAAAGCaaaGAAGCTTTGACAGAAGCACTTACTG	Mutation E88K
smFtsZmut-E86K-R13	CAGTAAGTGCTTCTGTCAAAGCTTCtttGCTTTCTTCAGCAGCTTTAC	
smFtsZmut-L268K-F15	GTCAATGTTACCGGCGGCaaaGATATGACGCTGACAGAAG	Mutation L269K
smFtsZmut-L268K-R15	CTTCTGTCAGCGTCATATCtttGCCGCCGGTAACATTGAC	

The cells were ruptured by high-pressure homogenization and centrifuged to collect the supernatant, which contained the expressed protein. The recombinant FtsZ was purified by following steps. First, the supernatant was flowed through a Ni^{2+}-NTA affinity column and eluted with Tris-HCl containing imidazole (300 mM). Second, Q-anion exchange chromatography was used to purify the proteins because the isoelectric point of FtsZ was about 4.3, and the proteins were eluted with a linear gradient of 0—1 M NaCl in 50 mM Tris-HCl buffer (pH 8.0).

The purified protein was eluted and concentrated with an ultrafiltration tube (30 KD). Then the concentrated protein was flowed through a size-exclusion chromatographic column (SuperdexTM 200) for final purification with 10 mM Tris-HCl (pH 8.0), 5 mM $MgCl_2$, and 150 mM KCl. Concentrated proteins were analyzed by sodium dodecyl sulfate (SDS)-polyacrylamide gel electrophoresis (PAGE) and quantitated by a BCA kit (Solarbio, China). Liquid nitrogen was used to quick freeze the protein, which was stored at −80°C.

2.8 | Western blot analysis

S. mutans FtsZ expression was detected by western blotting analysis. The protein concentration was measured using a BCA protein assay kit (Solarbio). Equal amounts of protein were separated by electrophoresis on 12% sodium dodecyl sulfate-polyacrylamide gel, then the gels were electroblotted onto polyvinylidene fluoride membranes (PVDF membranes; Bio-Rad, USA). The membranes were blocked for 60 min in 5% nonfat milk. After blocking, the membranes were incubated overnight with primary antibodies at 4°C. The primary antibodies used were custom-made antibody for *S. mutans* FtsZ (S-Evans Biosciences Ltd, Hangzhou, China) and anti-*S. mutans* (ABclonal ab31181, China). After being washed with PBS with 0.05% Tween, the membranes were incubated with secondary antibodies and detected by peroxidase-conjugated secondary antibodies (anti-rabbit IgG, Cell signaling Technology, USA) using the enhanced chemiluminescence system (NCM Biotech, China). The blots were scanned using a chemiluminescence scanner.

2.9 | FtsZ mutation construction

Clustal Omega was used to align the sequences of *S. mutans* FtsZ and *E. coli* FtsZ and to analyze the conserved amino acids. The pET28a-SmFtsZ plasmid, as a template, was used to amplify the full-length fragments of distinct *S. mutans* FtsZ mutations by quick-change PCR. The *S.*

TABLE 3 Properties of all proteins expressed in this study

Protein	Molecular weight (Da)	Length (aa)	Isoelectric point	aa Position
S. mutans FtsZ	45742.03	434	4.3	
E. coli FtsZ	40324.04	383	4.51	
SmFtsZ_mut E88D	45728.97	434	4.05	Right surface
SmFtsZ_mut S110T	45757.02	434	4.06	GTPase pocket
SmFtsZ_mut N168D	45743.98	434	4.04	Left surface
SmFtsZ_mut N189D	45743.98	434	4.04	Back surface
SmFtsZ_mut Y247S	45666.89	434	4.06	Left surface
SmFtsZ_mut L269F	45777.01	434	4.06	Bottom surface
SmFtsZ_mut E88A	45684.96	434	4.08	Right surface
SmFtsZ_mut L269A	45642.88	434	4.08	Bottom surface
SmFtsZ_mut E88K	45742.05	434	4.11	Right surface
SmFtsZ_mut L269K	45758.01	434	4.09	Bottom surface

mutans FtsZ mutations were transformed into *E. coli* BL21 (DE3), then expressed, and purified to obtain proteins (properties of all proteins expressed in this study are listed in Table 3).

2.10 | GTPase activity

During GTP hydrolysis, the inorganic phosphate is released proportionally. Thus, the amount of inorganic phosphate was detected by a malachite green dye-based reporter (Sundararajan et al., 2015). FtsZ was diluted in polymerization buffer ($MgCl_2$ 5 mM, KCL 150 mM, and buffer solution 50 mM) with different pH levels in 96-well plates. When 1 mM GTP was added in, the hydrolysis reaction began. After 5 min, the reaction was stopped using a chromogenic reagent (MAK307-1KT, Sigma, USA). The phosphate was measured by a full-wavelength microplate reader at 620 nm.

2.11 | FtsZ assembly

For electron microscopic analysis, FtsZ and FtsZ mutants (10 μM) were polymerized for 15 min at room temperature in the presence of 5 mM Mg^{2+}, 150 mM KCl, and 2 mM GTP at different pH levels. Buffer solution contains Tris pH 7.5, MES pH 6.0, and citrate-Na pH 5.0. Samples were transferred onto a carbon-coated copper grid (300 mesh), negatively stained with 1% uranyl acetate, and examined under a transmission electron microscope (JEOL JEM-F200).

3 | RESULTS

3.1 | *Streptococcus mutans* had similar cell division progress in acidic and neutral environments

To assess the aciduric ability of *S. mutans*, we cultured *S. mutans* UA159 in CDY medium with different pH levels for 22 h. The growth curves and doubling times of *S. mutans* are shown in Figures 1a and b. In pH 7.4 medium, the doubling time was 50 min, and the doubling time increased as the medium pH was lowered. In pH 5.0 medium, the doubling time was increased by twice the time (119 min). After 17 h of cultivation, it reached the stationary phase. Even in the pH 4.5 medium, the proliferation of *S. mutans* could still be observed. Conversely, another early colonizer of the tooth surface, *S. gordonii* ATCC 10558, showed a dramatically lower growth rate and final cell concentration in pH 5.0 medium. In acidic media with different pH levels, the growth of *S. gordonii* was significantly inhibited (Supporting information Figure S1). The growth rate of *S. mutans* was faster than that of *S. gordonii* in acidic media (pH 6.0, 5.5, 5.0, and 4.5).

Next, we checked the morphology of planktonically grown cells at pH 5.0 and 7.4. The results showed that compared with the neutral medium with pH 7.4, in the acidic medium with pH 5.0, the overall morphology of *S. mutans* cells did not change significantly, with all cells being round rod-shaped (Figure 1c). Furthermore, the cell length at pH 5.0 was longer than that at neutral pH (Figure 1d).

Furthermore, to study the effect of the acidic environment on the division of *S. mutans* cells during the exponential growth phase, we used transmission electron microscopy to observe the morphology of dividing cells. Images showed that cytokinesis was uniform, and that the division position tended to be in the middle of the two dividing cells (Figure 1e). The results showed that compared to *S. gordonii*, *S. mutans* was more acid tolerant. In addition, the morphology of *S. mutans* cells was ordinary in the acidic environment.

3.2 | *Streptococcus mutans* FtsZ showed full function in the acidic environment

To determine whether *S. mutans* FtsZ is functioned at pH 5.0, Western blot was used to investigate the expression level of *S. mutans* FtsZ in different pH media. A custom-made anti-*S. mutans* FtsZ antibody was

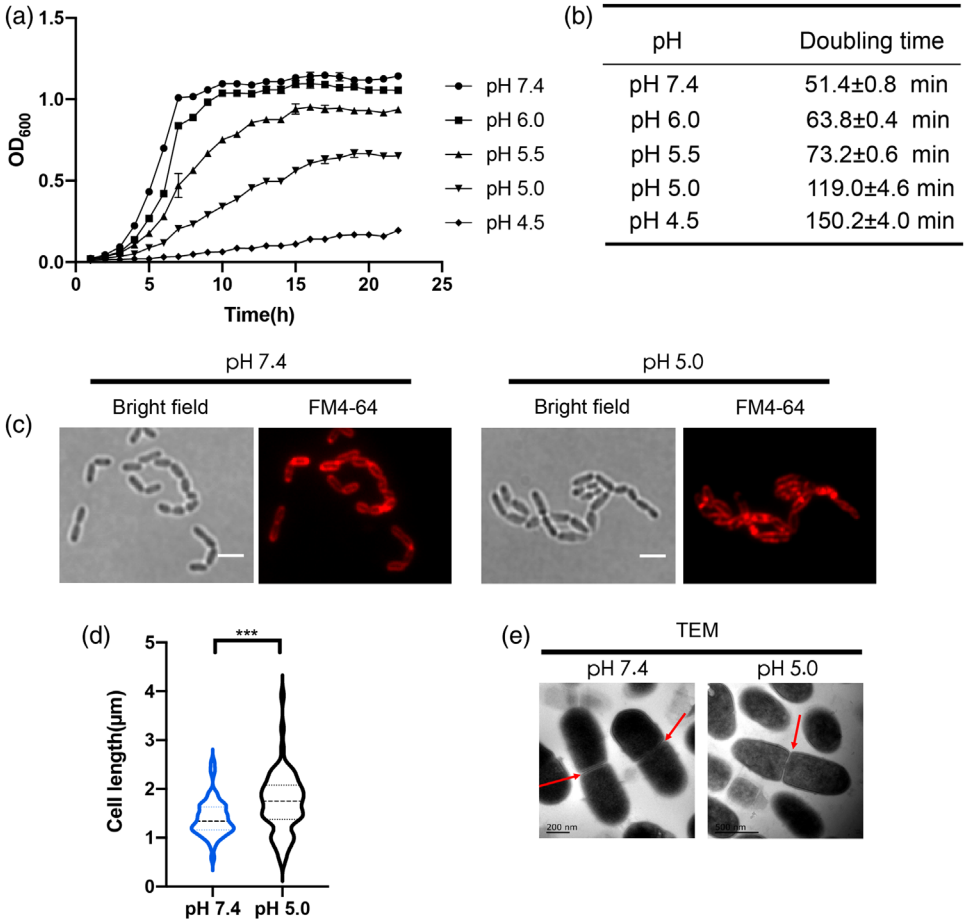

FIGURE 1 Effects of an acidic environment on *S. mutans* UA159 cells. (a) Growth curves of *S. mutans* UA159 at different pH levels. Data were obtained from three independent experiments. (b) Doubling times of different pH conditions calculated on the basis of the growth curves. Results are presented as mean ± SD. (c) Bright field and fluorescent scanning electron microscope images of *S. mutans* cells at pH 7.4 and 5.0 during the exponential growth phase. (d) Length measurements of bacterial cells at pH 7.4 (n = 103) and pH 5.0 (n = 71). *** represents $p<0.001$ (Mann–Whitney U test). (e) Transmission electron microscope images of *S. mutans* cells at pH 7.4 and 5.0 during the exponential growth phase. The red arrow marks the location of cell division. Representative images are shown.

used in the Western blot assay. Meanwhile, the anti-*S.mutans* antibody was used as a control. The expression level of FtsZ at pH 5.0 was similar to that at pH 7.4 (Figure 2a), suggesting that the expression level of FtsZ was not affected by the acidic environment.

We next studied the location of FtsZ via fluorescent microscopy (Figure 2b). The results showed that in the acidic medium with a pH value of 5.0, the main distribution area of the green fluorescence (*S. mutans* FtsZ) was not different compared to the neutral medium. The fluorescence was all located in the middle of the *S. mutans* cells, showing that the FtsZ formed Z-rings and involved in cell division.

Under TIRF imaging conditions, we investigated the dynamics of FtsZ in cells. The results showed that the fluorescence intensity of the Z-rings periodically fluctuated. There was no significant difference in cycle time between the acidic and neutral environments (~45 s for both; Figure 2c and d). Using a kymograph to measure the fluorescence intensity in the Z-ring, we could intuitively see the directional movement of FtsZ in the Z-rings (Figure 2e). Further quantification (velocity distribution measurements) by ImageJ showed that the *S. mutans* FtsZ had similar velocity distribution at either pH 7.4 or 5.0 environment (Figure 2f).

3.3 | *Streptococcus mutans* FtsZ had higher GTPase and assembly activity in pH 6.0 buffer than in the neutral environment

FtsZ, as a GTPase, can hydrolyze GTP to produce GDP and inorganic phosphate. We determined the GTP hydrolysis rate of *S. mutans* FtsZ (Figure 3a) and *E. coli* FtsZ (Supporting information Figure S2) at different pH levels (pH 4.0–7.4) using a malachite green assay to detect inorganic phosphate. When the pH value decreased, the GTP hydrolysis rate of *E. coli* FtsZ GTPase also decreased, which is consistent with previous studies (Mendieta et al., 2009).

Interestingly, *S. mutans* FtsZ had a relatively high GTP hydrolysis rate in the acidic environment, with the highest rate at pH 6.0 (Figure 3a). Furthermore, electron microscopy was used to identify differences in *S. mutans* FtsZ polymers between neutral and acidic poly-

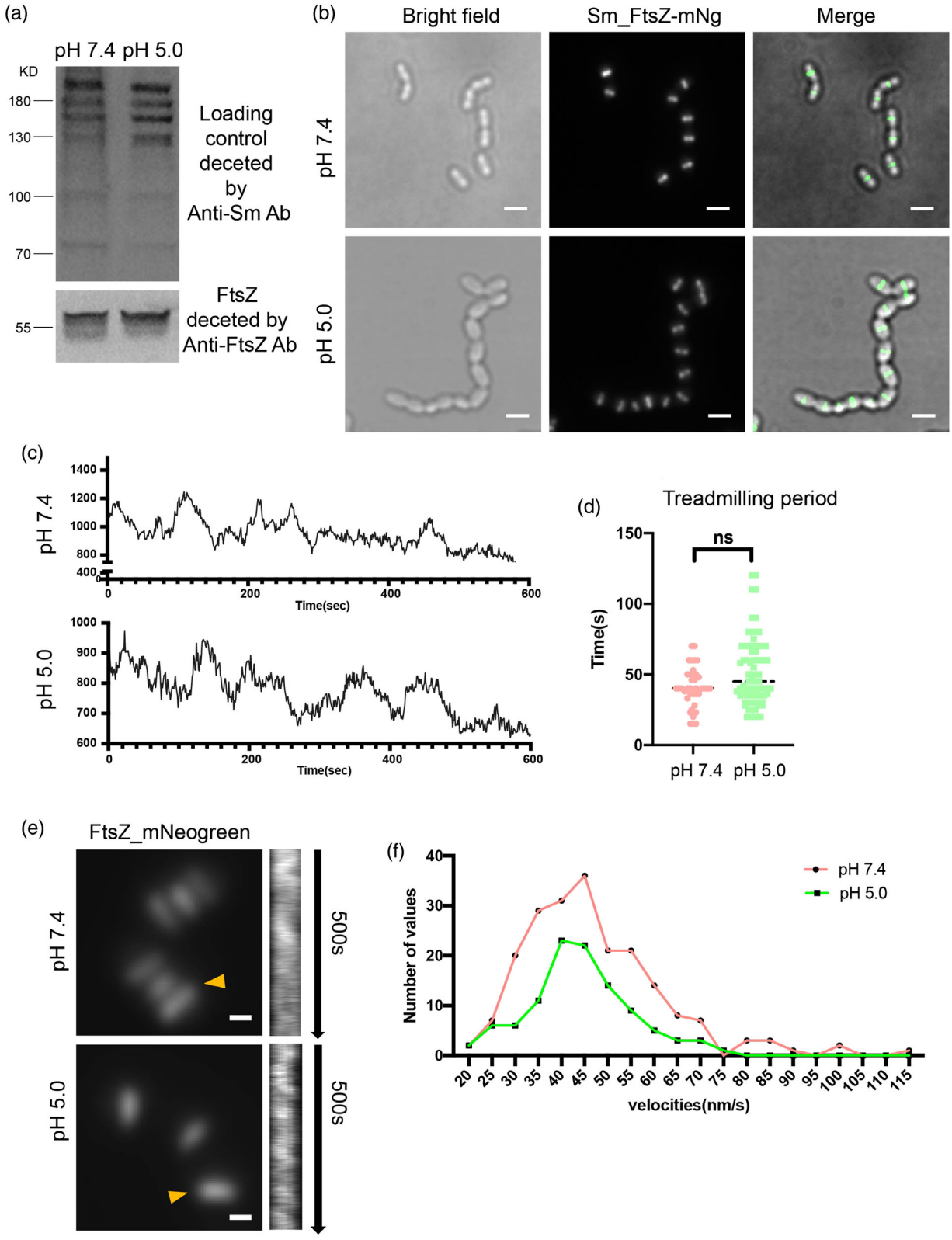

FIGURE 2 Characterization of *S. mutans* FtsZ in cells. (a) Western blot using anti-*S. mutans* antibody and anti-*S. mutans* FtsZ antibody. (b) Representative images of FtsZ rings in cells at pH 7.4 and 5.0. Cells expressing *S. mutans* FtsZ_mNeongreen (green) were analyzed by fluorescence microscopy. Scale bar, 2 μm. (c) Representative fluorescence intensity time traces of FtsZ rings at pH 7.4 and 5.0. (d) Tread milling period of cells at pH 7.4 (n = 206) and pH 5.0 (n = 105) were analyzed, respectively. $p = 0.0724$ (Mann–Whitney U test). (e) The use of FtsZ_mNeongreen revealed directional movement of FtsZ rings in cells at pH 7.4 and 5.0. The kymographs show the movement of FtsZ filaments inside the Z-rings (yellow arrows). (f) Distribution of the velocity of FtsZ filament movement inside the Z-rings of cells at pH 7.4 and 5.0. A total of 206 and 105 motion events were analyzed for pH 7.4 and 5.0, respectively

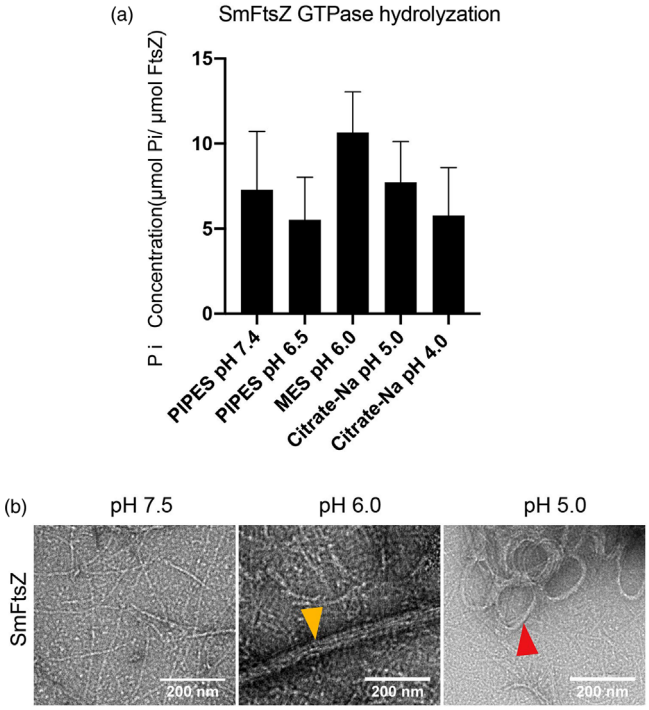

FIGURE 3 Effects of pH on FtsZ GTPase activity and polymerization. (a) GTPase activity of purified *S. mutans* FtsZ at different pH values. (b) Representative electron microscopy images of FtsZ polymers. FtsZ (10 mM) was incubated in the polymerization buffer (pH 7.5, 6.0, and 5.0) for 15 min with GTP (2 mM). The samples were negatively stained with 1% uranyl acetate. Scale bar, 200 nm. The filaments bundles were marked by yellow arrowhead. At pH 5.0, most of the bundles were circular (red arrowhead)

merization buffers. At pH 7.5, *S. mutans* FtsZ polymerized and produced protofilaments with an average length of 243.2 ± 147.2 nm and an average diameter of 8.628 ± 2.64 nm (n = 102) (Figure 3b). The filaments formed at pH 6.0 consisted of a dense network of protofilaments. A number of the filaments were long and highly laterally associated, forming straight, thick bundles with an average diameter of 54.42 ± 26.24 nm (n = 4). The length of the bundles extended past the microscopic field of view, as they were longer than 1442 nm (Figure 3b, yellow arrowhead). At lower pH values (pH 5.0), the trend of assembling thick bundles became more prominent. The difference was that most of the bundles at pH 5.0 were circular (red arrowhead). The protofilaments assembled by residual *S. mutans* FtsZ were significantly shorter, with an average length of 112.5 ± 40.53 nm (n = 104).

3.4 | Amino acids on the surface of *S. mutans* FtsZ are crucial to acidic tolerance

Unlike the in-depth study of the model organism *E. coli* FtsZ, *S. mutans* FtsZ showed strong acid resistance in vitro. The sequence alignment of *S. mutans* FtsZ and *E. coli* FtsZ made by Clustal Omega website is shown in Supporting information Figure S3A. Their identity of two proteins is 54.9%. The conserved residues between them were similar. Lu et al. has tested 16 site-directed mutants of *E. coli* FtsZ for assembly activity in vitro (Lu et al., 2001). Several of these sites had significantly reduced in vitro assembly activity, suggesting that they are essential for FtsZ function. By aligning *S. mutans* FtsZ and *E. coli* FtsZ sequences, six distinctive residues were identified. These residues were mutated to their respective conserved residues in *E. coli* FtsZ, and we studied their influence on assembly activity. Accordingly, six mutants were designed, namely, E88D, S110T, N168D, N189D, Y247S, and L269F.

The modeled structure of *S. mutans* FtsZ was simulated with the Robetta server (Baek et al., 2021). All of the amino acid positions of the mutations in the modeled structure of *S. mutans* FtsZ are shown in Figure 4a. If the FtsZ model was thought of as a cube, it would have six faces. The top and bottom faces of the subunit, which we called longitudinal, contacted subunits above and below it in the protofilament; the right and left faces, which we called lateral, contacted subunits adjacent to the protofilaments. We also had front and back surfaces. E88D was on the right surface of the cube. S110T was in the GTPase pocket. N168D and Y247S were on the left surface of the cube. N189D was on the back surface. L269F was on the bottom surface. Supporting information Figure S3B summarizes all these mutants of *S. mutans* FtsZ.

The presence of polymers was also verified by electron microscopy. A cluster of mutations (S110T, N168D, N189D) showed similar polymerization activity with wild-type *S. mutans* FtsZ (Supporting information Figure S4). In the neutral environment (pH 7.5), *S. mutans* FtsZ filaments were visible, seeming to have interwoven networks rather than bundles. The protofilaments formed at pH 6.0 consisted of a dense network of protofilaments that were long and highly laterally associated (thick bundles). At pH 5.0, *S. mutans* FtsZ mutants assembled into protofilaments and filament bundles that formed closed circular hoops. Y247S showed a similar assembly form in an acid environment at pH 6.0 and 5.0. Nevertheless, there were no polymers in the neutral environment (Supporting information Figure S4).

E88D and L269F were significantly affected in terms of polymer assembly (Figure 4b). At pH 7.5, almost no polymerization was observed. At pH 6.0, a network of protofilaments was observed. Several of the protofilaments assembled some twin protofilaments rather than thick bundles. At pH 5.0, the polymers of these mutants were shorter and less dense compared with those of the wild-type *S. mutans* FtsZ. It was presumed that E88 and L269 are critical for *S. mutans* FtsZ assembly. Furthermore, E88 and L269 were substituted to K and A, respectively. Accordingly, four mutants were designed, namely, E88A, E88K, L269A, and L269K. The assembly activity of all these mutants was recovered to some extent (Figure 4c). Sparse protofilaments of E88A and L269A were found in an environment at pH 7.5. In an acid environment (pH 6.0 and pH5.0), both E88A and L269A recover the ability to form protofilaments. However, we did not detect the filament bundle at pH 6.0. The filament bundles (circular hoops) were observed until the pH decreased to 5.0.

Interestingly, when E88 and L269 were mutated to alkaline amino acids K, the mutation proteins could not assemble into filament bundles even at pH 5.0 (Figure 4c), indicating a lower polymerization ability of E88K and L269K. These data suggest that E88 and L269 are the crucial sites of response to pH changes.

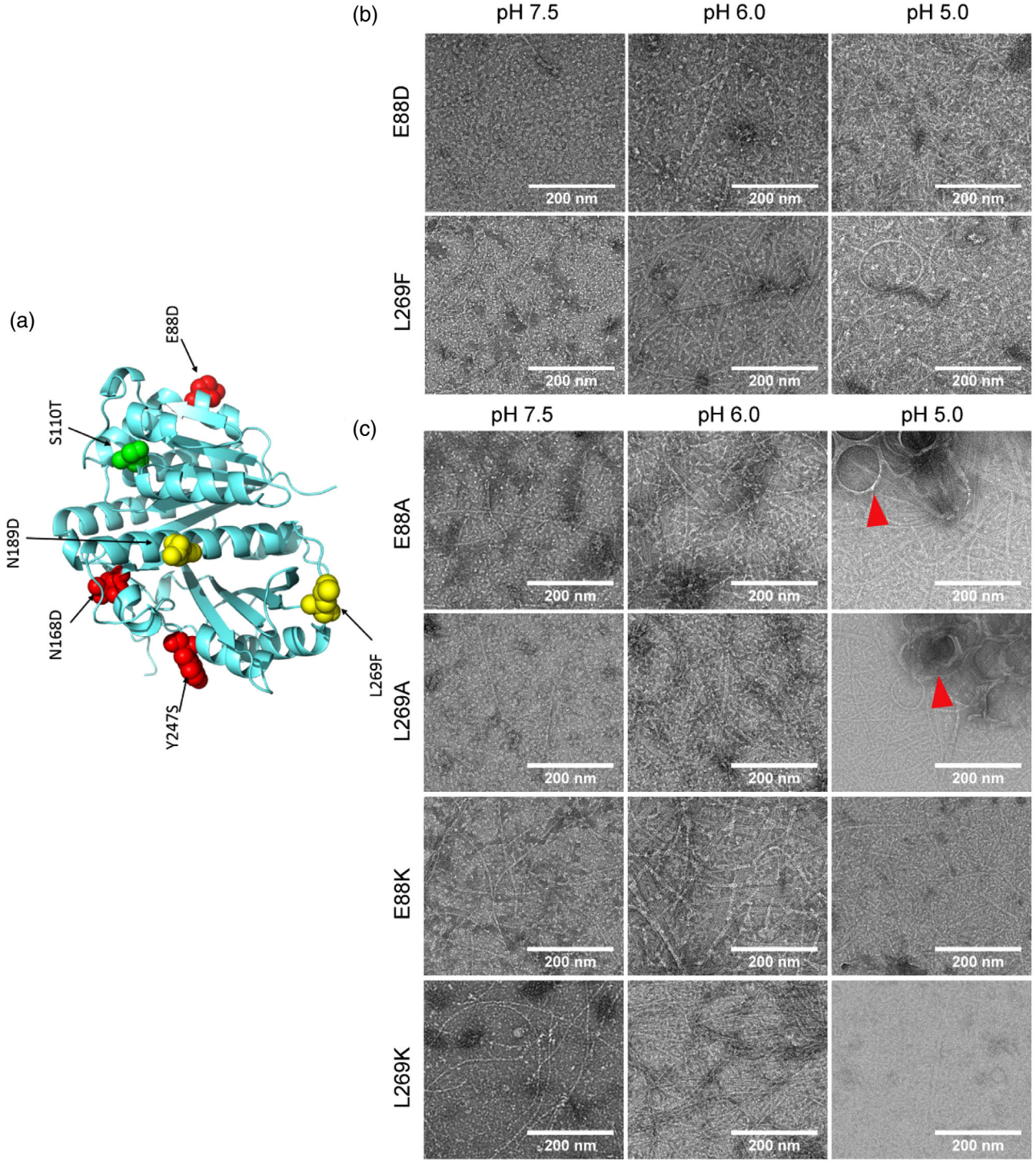

FIGURE 4 Filament polymerization capabilities of *S. mutans* FtsZ mutations evaluated by electron microscopy in vitro. (a) All *S. mutans* FtsZ mutation positions are shown in this modeled structure of *S. mutans* FtsZ. Thinking of the FtsZ model was thought of as a cube, it has six faces. E88D was on the right surface. S110T was in the GTPase pocket. N168D and Y247S were on the left surface. N189D was on the back surface. L269F was on the bottom surface. (b) Effect of pH on the polymerization of *S. mutans* FtsZ mutations. E88D and L269F (10 mM) were incubated in the polymerization buffer (pH 7.5, 6.0, and 5.0) for 15 min with GTP (2 mM). The samples were negatively stained with 1% uranyl acetate. Scale bar, 200 nm. (c) Effect of pH on the polymerization of *S. mutans* FtsZ mutations (E88A, E88K, L269A, and L269K). *Streptococcus mutans* FtsZ mutations (10 mM) were incubated in the polymerization buffer (pH 7.5, 6.0, and pH 5.0) for 15 min with GTP (2 mM). The samples were negatively stained with 1% uranyl acetate. Scale bar, 200 nm. E88A and L269A assembled into protofilaments and filament bundles that formed closed circular hoops (red arrowhead) at pH 5.0

4 | DISCUSSION

Recently, most relevant research has focused on the cell division of *Streptococci* because these bacteria differ from any other established bacterial models in terms of cytokinesis (Fleurie et al., 2014; Teeseling et al., 2017). However, very little is currently known about how an acidic environment affects *S. mutans* cell division.

The results of the present study showed that *S. mutans* cell division progress in an acidic environment was similar to that in a neutral environment. The splitting position was in the middle of cells, and the cytoplasm was divided evenly in the acidic environment. These results further support the idea that *S. mutans* has a remarkable ability to withstand the acid onslaught by using a wide variety of highly evolved acid-tolerance mechanisms including macromolecule protection, metabolism alteration, and intracellular pH homeostasis. Despite possessing a complex and sophisticated means of regulating an environment of acidic stress, the intracellular environment of *S. mutans* remains acidic (Iwami et al., 2002). This study focused on whether the core protein of cell division could maintain function in cells in an acidic extracellular environment.

The FtsZ protein, a homolog of microtubulin, can hydrolyze GTP and polymerize itself by binding GTP in vitro and in vivo. FtsZ is the first protein to localize at the site of bacterial cytokinesis in most of the bacteria that have been studied so far, with FtsZ polymerizing to form a ring-like structure, known as the Z-ring. The Z-ring is then used as a scaffold to recruit other division-related proteins, both cytoplasmic and endosomal or intermembrane, to complete the cell division process.

The results of the present study showed that FtsZ was correctly localized in the acidic environment; Z-rings were formed, and protein expression levels were not reduced. On the other hand, previous studies have shown that the movement period and tread milling velocity of FtsZ are closely related to protein function. In this study, the movement cycle and tread milling velocity of *S. mutans* FtsZ in the middle of cells were not impaired in the acidic environment, suggesting that *S. mutans* FtsZ was fully functional at low pH in vivo. Given this result, together with the previous findings that the intracellular pH of *S. mutans* is acidic, our hypothesis was that *S. mutans* FtsZ has acidic tolerance, unlike FtsZ from other model organisms.

To verify our hypothesis, we further assessed the protein function again in vitro. *Streptococcus mutans* FtsZ had higher GTPase activity at pH 6.0 buffer than in the neutral environment. This result is different from the *E. coli* FtsZ properties shown in previous experiments. Mendieta et al. measured the GTPase activity of *E. coli* FtsZ in vitro over a wide range of pH values (4.8–8.0); the GTPase activity values significantly decreased when the pH changed from 7.0 to 6.0 and became undetectable when the pH values was lower than 5.5 (Mendieta et al., 2009).

The hydrolysis reaction of GTPase occurs by the FtsZ polymerization reaction (Erickson et al., 2010). Therefore, electron microscopy was performed to identify differences in *S. mutans* FtsZ polymers between neutral and acidic polymerization buffers. The protofilaments formed at pH 6.0 consisted of a dense network of protofilaments and the long and highly laterally associated thick bundles. This result is consistent with the trend that GTPase activity is most significant at pH 6.0. We suspect that the most powerful activity of *S. mutans* FtsZ at pH 6.0 is also related to the intracellular environment of *S. mutans*, verifying our hypothesis that *S. mutans* FtsZ has a specific acid tolerance mechanism.

To further study the specific acid tolerance mechanism of *S. mutans* FtsZ, we constructed six site-directed mutants of *S. mutans* FtsZ. The mutated amino acids were all exposed on the surface. The examined mutations covered a range of surface areas of the *S. mutans* FtsZ molecule and may aid in elucidating the acid tolerance mechanism. Polymerization capacity is the functional basis of FtsZ. FtsZ assembly involves two types of polymerization. First, FtsZ assembles in an orientation similar to that of polymerized tubulin, with each FtsZ monomer maintaining head-to-tail interactions (Erickson et al., 1996). These head-to-tail interactions are referred to as longitudinal contacts and are the basis of protofilament formation. Another interaction is referred to as lateral contact, which functions to bring protofilaments together. Both interactions may play essential roles in Z-ring nucleation, assembly, regulation, and disassembly. In this study, three of the six mutants (S110T, N168D, N189D) showed apparently normal assembly in the neutral and acidic environments. Like Lu et al., we found that FtsZ protofilaments could adopt either a straight or curved conformation (Lu et al., 2000). The straight and curved conformations are favored by GTP and GDP, respectively (Lu et al., 2001). In the present study, curved conformations, especially the circle filaments, appeared frequently in the acidic environment (pH 5.0). Another study has proposed that the hydrolysis of GTP results in a substantial movement of the T3 loop and that this movement might be involved in the transition to the curved conformation (Dıáz et al., 2001). Therefore, whether the curved conformation is due to a decrease in GTPase activity in an acidic environment needs further investigation.

The polymers of mutants at positions E88 and L269 showed pH-dependent changes. Furthermore, it was difficult to find polymers bundles in the pH 5.0 environment for E88K and L269K. According to the protein simulation structure, L269 was located on the synergy T7 loop of *S. mutans* FtsZ. The longitudinal interface contained the GTPase active site. In this area, the synergy T7 loop in the C-terminal domain of one FtsZ monomer was inserted into the nucleotide-binding pocket of the N-terminal domain of the adjacent molecule. Additionally, E88, the amino acid site located on the lateral surface of *S. mutans* FtsZ, displayed an equally important role in FtsZ polymerization. Consequently, the L269K and E88K polymers showed that the longitudinal and lateral interfaces may play significant roles in responding to the acidic environment.

5 | CONCLUSIONS

In conclusion, our results showed that *S. mutans* presented similar cell division progress in acidic and neutral environments. FtsZ was first localized to the bacterial cell division site and is a core protein in the division complex. The present research first evaluated the perfor-

mance of *S. mutans* FtsZ at different pH levels in vivo. The acidic environment did not affect the position, expression level, and tread milling velocity of *S. mutans* FtsZ. Second, *S. mutans* FtsZ exhibited higher functional activity in the acidic environment than in the neutral environment in vitro. Unlike *E. coli* FtsZ, we believe that *S. mutans* FtsZ may have the special property of acid tolerance. Despite the fact that the protein structure of *S. mutans* FtsZ was not clarified, we established the sequence alignment of *S. mutans* FtsZ and *E. coli* FtsZ via the Clustal Omega website. Several distinctive residues among them were selected to change. We have tested 10 site-directed mutants of *S. mutans* FtsZ for assembly, and the results were verified by electron microscopy in vitro. Interestingly, the polymerization of E88 and L269 changed depending on the different pH environments, suggesting that E88 and L269 are the crucial sites of response to pH changes. However, further studies are needed to clarify the structure of *S. mutans* FtsZ to elucidate the acid resistance mechanism.

ACKNOWLEDGMENTS

This work was supported by the National Natural Science Foundation of China (81991501, and 82001039), China Postdoctoral Science Foundation (No. 2020M680265), Beijing Natural Science Foundation : 7222220, and Young Elite Scientist Sponsorship Program by CAST (No. 2019QNRC001 to YL.L). We thank the Core Facilities of Life Sciences and National Center for Protein Sciences at Peking University in Beijing, China, for assistance with TEM imaging and we would be grateful to Yiqun Liu for his help of taking images.

CONFLICT OF INTEREST

The authors have no competing financial interest to declare.

DATA AVAILABILITY STATEMENT

The data that support the findings of this study are available from the corresponding author upon reasonable request.

PEER REVIEW

The peer review history for this article is available at https://publons.com/publon/10.1111/omi.12364.

ORCID

Yongliang Li https://orcid.org/0000-0001-5016-2778

REFERENCES

Baek, M., DiMaio, F., Anishchenko, I., Dauparas, J., Ovchinnikov, S., Lee, G. R., Wang, J., Cong, Q., Kinch, L. N., Schaeffer, R. D., Millán, C., Park, H., Adams, C., Glassman, C. R., DeGiovanni, A., Pereira, J. H., Rodrigues, A. V., van Dijk, A. A., Ebrecht, A. C., … , & Baker, D. (2021). Accurate prediction of protein structures and interactions using a three-track neural network. *Science*, *373*(6557), 871–876. https://doi.org/10.1126/science.abj8754

Baker, J. L., Faustoferri, R. C., & Quivey, R. G. (2017). Acid-adaptive mechanisms of *Streptococcus mutans*—the more we know, the more we don't. *Molecular Oral Microbiology*, *32*(2), 107–117. https://doi.org/10.1111/omi.12162

Bender, G. R., Sutton, S. V. W., & Marquis, R. E. (1986). Acid tolerance, proton permeabilities, and membrane ATPases of oral streptococci. *Infection and Immunity*, *53*(2), 331–338. https://doi.org/10.1128/iai.53.2.331-338.1986

Bramhill, D., & Thompson, C. M. (1994). GTP-dependent polymerization of *Escherichia coli* FtsZ protein to form tubules. *Proceedings of the National Academy of Sciences of the United States of America*, *91*(13), 5813–5817. https://doi.org/10.1073/pnas.91.13.5813 https://doi.org/10.1073/pnas.91.13.5813

De, A., Jorgensen, A. N., Beatty, W. L., Lemos, J., & Wen, Z. T. (2018). Deficiency of MecA in *Streptococcus mutans* causes major defects in cell envelope biogenesis, cell division, and biofilm formation. *Frontiers in Microbiology*, *9*, 2130. https://doi.org/10.3389/fmicb.2018.02130

De Boer, P., Crossley, R., & Rothfield, L. (1992). The essential bacterial cell-division protein FtsZ is a GTPase. *Nature*, *359*(6392), 254–256. https://doi.org/10.1038/359254a0

Diáz, J. F., Kralicek, A., Mingorance, J., Palacios, J. M., Vicente, M., & Andreu, J. M. (2001). Activation of cell division protein FtsZ: control of switch loop T3 conformation by the nucleotide γ-phosphate*. *Journal of Biological Chemistry*, *276*(20), 17307–17315. https://doi.org/10.1074/jbc.M010920200

Erickson, H. P., Anderson, D. E., & Osawa, M. (2010). FtsZ in bacterial cytokinesis: cytoskeleton and force generator all in one. *Microbiology and Molecular Biology Reviews*, *74*(4), 504–528. https://doi.org/10.1128/MMBR.00021-10

Erickson, H. P., Taylor, D. W., Taylor, K. A., & Bramhill, D. (1996). Bacterial cell division protein FtsZ assembles into protofilament sheets and minirings, structural homologs of tubulin polymers. *Proceedings of the National Academy of Sciences of the United States of America*, *93*(1), 519–523. https://doi.org/10.1073/pnas.93.1.519

Fleurie, A., Lesterlin, C., Manuse, S., Zhao, C., Cluzel, C., Lavergne, J.-P., Franz-Wachtel, M., Macek, B., Combet, C., Kuru, E., VanNieuwenhze, M. S., Brun, Y. V., Sherratt, D., & Grangeasse, C. (2014). MapZ marks the division sites and positions FtsZ rings in *Streptococcus pneumoniae*. *Nature*, *516*(7530), 259–262. https://doi.org/10.1038/nature13966

Iwami, Y., Kawarada, K., Kojima, I., Miyasawa, H., Kakuta, H., Mayanagi, H., & Takahashi, N. (2002). Intracellular and extracellular pHs of *Streptococcus mutans* after addition of acids: loading and efflux of a fluorescent pH indicator in *Streptococcal* cells. *Oral Microbiology and Immunology*, *17*(4), 239–244. https://doi.org/10.1034/j.1399-302X.2002.170406.x

Lemos, J. A., Palmer, S. R., Zeng, L., Wen, Z. T., Kajfasz, J. K., Freires, I. A., Abranches, J., & Brady, L. J. (2019). The biology of *Streptococcus mutans*. *Microbiology Spectrum*, *7*(1),. https://doi.org/10.1128/microbiolspec.GPP3-0051-2018

Lu, C., Reedy, M., & Erickson, H. P. (2000). Straight and curved conformations of FtsZ are regulated by GTP hydrolysis. *Journal of Bacteriology*, *182*(1), 164–170. https://doi.org/10.1128/JB.182.1.164-170.2000

Lu, C., Stricker, J., & Erickson, H. P. (2001). Site-specific mutations of FtsZ—effects on GTPase and in vitro assembly. *BMC Microbiology*, *1*(1), 1–12. https://doi.org/10.1186/1471-2180-1-7

Lund, P., Tramonti, A., & De Biase, D. (2014). Coping with low pH: molecular strategies in neutralophilic bacteria. *FEMS Microbiology Reviews*, *38*, 1091–1125. https://doi.org/10.1111/1574-6976.12076

Mahone, C. R., & Goley, E. D. (2020). Bacterial cell division at a glance. *Journal of Cell Science*, *133*(7), jcs237057. https://doi.org/10.1242/jcs.237057

Matsui, R., & Cvitkovitch, D. (2010). Acid tolerance mechanisms utilized by *Streptococcus mutans*. *Future Microbiology*, *5*, 403–417. https://doi.org/10.2217/fmb.09.129

Mendieta, J., Isabel Rico, A., López-Viñas, E., Vicente, M., Mingorance, J., & Gómez-Puertas, P. (2009). Structural and functional model for ionic (K^+/Na^+) and pH dependence of GTPase activity and polymerization of FtsZ, the prokaryotic ortholog of tubulin. *Journal of Molecular Biology*, *390*, 17–25. https://doi.org/10.1016/j.jmb.2009.05.018

Mueller, E. A., Westfall, C. S., & Levin, P. A. (2019). Environmental pH impacts division assembly and cell size in *Escherichia coli*. *BioRxiv*, *747808*. https://doi.org/10.1101/747808 bioRxiv

Nogales, E., Downing, K. H., Amos, L. A., & Löwe, J. (1998). Tubulin and FtsZ form a distinct family of GTPases. *Nature Structural Biology*, *5*(6), 451–458. https://doi.org/10.1038/nsb0698-451

Slonczewski, J. L., Rosen, B. P., Alger, J. R., & Macnab, R. M. (1981). pH homeostasis in Escherichia coli: measurement by 31P nuclear magnetic resonance of methylphosphonate and phosphate. Proceedings of the National Academy of Sciences of the United States of America, *78*(10I), 6271–6275. https://doi.org/10.1073/pnas.78.10.6271

Sundararajan, K., Miguel, A., Desmarais, S. M., Meier, E. L., Casey Huang, K., & Goley, E. D. (2015). The bacterial tubulin FtsZ requires its intrinsically disordered linker to direct robust cell wall construction. *Nature Communications*, *6*(1), 1–14. https://doi.org/10.1038/ncomms8281

Teeseling, M. C. F. van, Pedro, M. A. de, & Cava, F. (2017). Determinants of bacterial morphology: from fundamentals to possibilities for antimicrobial targeting. *Frontiers in Microbiology*, *8*, 1264. https://doi.org/10.3389/fmicb.2017.01264

Van De Rijn, I., & Kessler, R. E. (1980). Growth characteristics of group A *streptococci* in a new chemically defined medium. *Infection and Immunity*, *27*(2), 444–448. https://doi.org/10.1128/IAI.27.2.444-448.1980

Xie, Z., Okinaga, T., Qi, F., Zhang, Z., & Merritt, J. (2011). Cloning-independent and counterselectable markerless mutagenesis system in *Streptococcus mutans*. *Applied and Environmental Microbiology*, *77*(22), 8025–8033. https://doi.org/10.1128/AEM.06362-11

Yang, X., Lyu, Z., Miguel, A., McQuillen, R., Huang, K. C., & Xiao, J. (2017). GTPase activity-coupled treadmilling of the bacterial tubulin FtsZ organizes septal cell wall synthesis. *Science*, *355*(6326), 744–747. https://doi.org/10.1126/science.aak9995

SUPPORTING INFORMATION

Additional supporting information may be found in the online version of the article at the publisher's website.

How to cite this article: Chen, Y., Li, Y., Yuan, C., Liu, S., Xin, F., Deng, X., & Wang, X. (2022). *Streptococcus mutans* cell division protein FtsZ has higher GTPase and polymerization activities in acidic environment. *Molecular Oral Microbiology*, *37*, 97–108. https://doi.org/10.1111/omi.12364